

Lidar Remote Sensing In Atmospheric and Earth Sciences

Dr. C. Russell Philbrick
Prof. Electrical & Computer Eng.
Communications & Space Sci. Lab
Pennsylvania State University
315 Electrical Engineering East
University Park, PA 16802

(O) 814-865-2975 (H) 814-867-7298
PENNSTATE FAX (814) 863-7005
 CRP@ECL.PSU.EDU.

Reviewed and revised papers presented at the
twenty-first International Laser Radar Conference
(ILRC21)
Québec, Canada
8 - 12 July 2002

Luc R. Bissonnette, Gilles Roy, and Gilles Vallée
Editors

Luc Bissonnette
Gilles Roy
Gilles Vallée

Defence R&D Canada – Valcartier
Val-Bélair, Québec
Canada

Type setting : Electronic files or camera ready paper copies submitted by the authors

Cover page: Time-height and range-height plots of lidar returns from rainfall,
courtesy of Gilles Roy, DRDC Valcartier. Picture of weather clouds
obtained from © Gregory Thompson www.inclouds.com

Cover design: Jocelyne Audy, Defence R&D Canada – Valcartier

Available from: Library Services
Defence R&D Canada - Valcartier
2459 Pie-XI Blvd North
Val-Bélair, QC G3J 1X5
Canada

Raman Lidar Descriptions of Lower Atmosphere Processes

C. Russell Philbrick
Penn State University
Department of Electrical Engineering
University Park PA 16802
Tel: 814-865-2975 • Fax: 815-863-8457
Email: crp3@psu.edu

ABSTRACT

Raman lidar provides vertical profiles of most of the key parameters needed to analyze and forecast the meteorological conditions, and to investigate processes controlling air quality in the lower atmosphere. The time sequence of atmospheric profiles is most valuable in understanding the meteorological processes controlling the evolution of air pollution events. The vibrational and rotational Raman lidar signals provide simultaneous profiles of meteorological parameters of temperature and water vapor, as well as the air quality parameters of ozone and airborne particulate matter. The LAPS (Lidar Atmospheric Profile Sensor) developed in 1995 was the first operational prototype Raman lidar instrument. It makes use of 2nd and 4th harmonic generated laser beams of a Nd:YAG laser to provide both daytime and nighttime measurements of atmospheric properties. The Raman scatter signals from vibrational states of water vapor and nitrogen provide robust profiles of the specific humidity in the lower atmosphere. The temperature profiles are measured using the ratio of rotational Raman signals at 530 and 528 nm, and the temperature profile is combined with the specific humidity measurements to calculate profiles of relative humidity and RF refractivity. In addition, profiles of optical extinction are determined from the gradients in the measured profiles of each of several molecular profiles. Wavelengths at 284 nm, 530 nm and 607 nm are used routinely to determine profiles of optical extinction. The ozone profiles in the lower troposphere are measured using a DIAL analysis of the ratio of the vibrational Raman signals from nitrogen (284 nm) and oxygen (278 nm), which are on the steep side of the Hartley band of ozone. Examples from several data sets are provided to demonstrate the utility of Raman lidar as a tool to provide the data needed by the meteorology and air quality communities, and to show the improved level of understanding of atmospheric processes that is gained from applications of lidar techniques.

1. INTRODUCTION

Measurements of the meteorological properties serve a vital role in modeling and forecasting weather conditions that impact many aspects of our daily lives. The meteorological conditions control the development and dissipation of air pollution episodes. Air pollution has been demonstrated to affect health, influence our activities due to changes in visibility, and is a focus of our concerns for the global environment. A better understanding of the variations in 'greenhouse gases' and particle concentrations that influence the Earth's radiation balance is needed. The two principal components of the atmosphere that have been singled out as major air pollution concerns are ozone and airborne particulate matter (PM). Airborne particulate matter has been shown to be associated with increased hospital admissions for cardiovascular disease.^{1,2} Ozone is a known toxic species that causes deleterious respiratory effects, particularly causing blisters in the respiratory tract, ageing of tissue and complications for older individuals, and those with asthma and other respiratory problems.^{3,4} The increase in airborne particulate matter has changed the optical properties of the atmosphere by decreasing visibility which directly affects air traffic patterns and landing frequency of commercial aircraft, and by reducing the aesthetic appreciation of our national parks.⁵ The increase of emissions into the atmosphere results in competing non-linear response mechanisms which affect the energy balance that controls our global climate: 1) increased emission of chemical species that absorb infrared radiation can lead to warming from the 'greenhouse' effect, 2) increased airborne particulate matter reduces direct and indirect flux of solar radiation leading to cooling from changes in the planetary albedo. The increase in airborne particulate matter is principally due to combustion products from transportation and power generation.⁴ Improved meteorological measurements with better temporal and spatial resolution are needed to model the complex atmospheric system with a coupled physics based model and real time data products. Raman lidar is proposed as the primary data source for future meteorological and air quality data.

The Raman lidar techniques outlined here are expected to provide an important tool to gain the understanding required to improve weather forecasts, and to predict and/or mitigate future air pollution episodes. Raman lidar is a robust tool that can be employed to measure a wide range of meteorological and environmental properties.⁶ The most important parameters for testing model calculations are the measured vertical profiles of water vapor, temperature, ozone and particulate matter. The general approach used in developing the data base for analysis and prediction has been based upon networks of ground sites that make local *in situ* measurements. Prior analysis has suffered from the fact that little information was obtained on the vertical structure because of the expense of using balloon and aircraft platforms to obtain measurements aloft. Raman lidar can provide continuous time sequences of the vertical profiles of the key parameters in the lower atmosphere. The examples of profiles shown here demonstrate the present capability for measuring the needed properties. The most important meteorological parameters are temperature and water vapor. Temperature is measured from the ratio of profiles of the rotational Raman signal intensity. The water vapor is determined from the specific humidity measured by the ratio of the vibrational Raman radiation scattered by water vapor and molecular nitrogen. The temperature and specific humidity profiles are combined to directly calculate two other useful parameters, the RF refractivity and the relative humidity. The ozone profiles in the lower atmosphere are measured directly from the absorption of the Raman scatter from nitrogen and oxygen at wavelengths in the Hartley band. The particulate matter is determined from the measurements of optical extinction and backscatter at visible and ultraviolet wavelengths. The water vapor is a particularly important tracer of the tropospheric dynamics and provides a marker of the thickness of the planetary boundary layer, thereby describing the dilution volume for the chemical species emitted into the atmosphere. The Raman lidar techniques used to investigate atmospheric processes are described in the following section.

2. RAMAN LIDAR MEASUREMENT TECHNIQUES

Raman scattering is one of the processes that occurs when optical radiation is scattered from the molecules of the atmosphere. It is very useful because the vibrational Raman scattering provides distinct wavelength shifts for species specific vibrational energy states of the molecules, additionally rotational Raman scattering provides signals with a wavelength dependence directly related to the atmospheric temperature.⁶ Figure 1(a) shows a diagram of the vibrational and rotational energy levels that are associated with Raman scatter. When a photon scatters from a molecule, the distribution of energy in the charge cloud results in a virtual energy state. Most of the atmospheric molecules reside in the ground vibrational level because the vibrational state excitation corresponds to relatively large energy transitions (tenths of eV for simple molecules like nitrogen and oxygen) compared to the thermal energy available. After scattering occurs, most of the events result in the return of the molecule to the ground state, and the emitted photon has the energy of the initial photon, plus/minus the random thermal velocity of the molecule, that is the Doppler broadening. A small fraction of the transitions (order of 0.1%) result in giving part of the photon energy to the molecule, and ending in the first vibrational level (a Stokes transition). The emitted photon energy is decreased by exactly the energy of the vibrational state quanta for that molecule. For the small fraction of molecules existing in the vibrational excited level, the unlikely anti-Stokes transition is possible. The relative intensities of the scattering signals are indicated by the scattering cross-section values at 532 nm in Figure 1(b). The wavelengths of vibrational Raman back scatter signals from the molecules of the water vapor and molecular nitrogen are widely separated from the exciting laser radiation and can be easily isolated for measurement using modern filter technology and sensitive photon counting detectors.⁷ The ratio of rotational Raman signals at 528 nm and 530 nm provides a measurement of atmospheric temperature.^{8,9} All of the molecules of the lower atmosphere are distributed in the rotational states according to the local temperature. By measuring the ratio of scattered signals at two wavelengths, the temperature can be directly measured. In order to push the lidar measurement capability into the daylight conditions, we use the "solar blind" region of the spectrum between 260 and 300 nm. The "solar blind" region is darkened by the stratospheric ozone absorption of ultraviolet radiation. Night time measurements are made using the 660nm/607nm (H_2O/N_2) signal ratio from the doubled Nd:YAG laser radiation at 532 nm. Daylight measurements are obtained using the 295nm/284nm (H_2O/N_2) ratio from the quadruple Nd:YAG laser radiation at 266 nm. A small correction for the tropospheric ozone must be applied. That correction can be obtained from measuring the ratio of the O_2/N_2 signals, 278nm/284nm. From this analysis, the ozone profiles in the lower troposphere are also obtained.¹⁰ The Raman techniques, which use ratios of the signals for measurement of water vapor and temperature, have the major advantage in removing essentially all of uncertainties, such as any requirement for knowledge of the absolute sensitivity and non-linear factors.¹¹ The measurement parameters can be uniquely determined from knowledge of the laboratory Raman cross-sections. Optical extinction is measured using the gradient of the measured molecular profile compared with that expected for the density gradient of the lower atmosphere.¹²⁻¹⁶

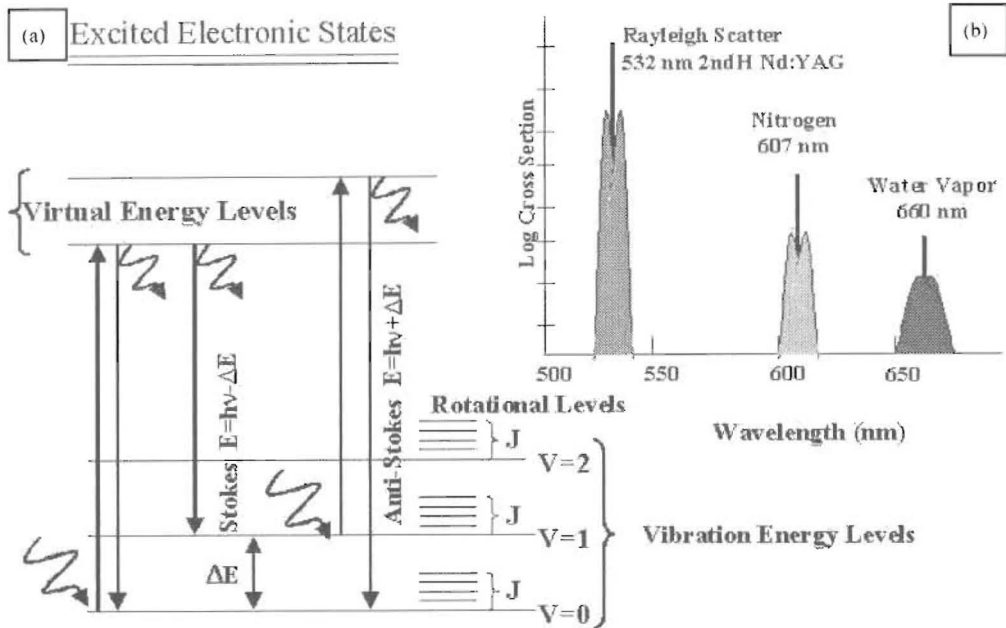


Figure 1. (a) The energy diagram of a molecule illustrates that the scattering of a photon raises the molecule to a virtual level which normally decays to ground ($V=0$) emitting a photon of the same energy as the incident energy, only broadened by thermal Doppler velocity. In a small fraction of cases, the scattered photon is Raman shifted to the first vibrational level ($V=1$), a Stokes shift. The relatively large vibrational energy (ΔE) compared with thermal energy makes the anti-Stokes vibrational transition unlikely. The rotational states (J -levels) are populated by thermal excitation in both Stokes and anti-Stokes branches. (b) The relative intensities of the Stokes vibrational Raman shifts of oxygen, nitrogen and water vapor are indicated for scattering from atmospheric molecules with the double Nd:YAG laser at 532 nm. The distributions of relative rotational states are indicated by envelopes of the individual lines.^{6,9}

2.1. Water Vapor Measurements

The specific humidity, or water vapor mixing ratios, are determined by taking the ratio of the signals from the 1st Stokes vibrational Raman shifts for water vapor and nitrogen. The measurements are made with laser lines at visible (532 nm) and ultraviolet (266 nm) wavelengths. The visible measurements (660/607) are available at night and the ultraviolet measurements (294/284) are available day and night. The ultraviolet profiles are limited to the first 3 km because of signal attenuation due to the large scattering cross-section. The ultraviolet water vapor instrument calibration value has remained relatively constant for the LAPS instrument during the past six years, however the visible sensitivity has shown significant changes, possibly due to sometime overloads the photomultiplier tube during daylight. Investigation of the stability of the instrument has shown that the differences between the water vapor measurements using the meteorological balloon sonde and the lidar are about $\pm 4\%$, and this is approximately the value of variations expected due to the atmospheric spatial and temporal differences.¹⁶

2.2. Ozone Measurements

The Raman vibrational 1st Stokes shifts from molecular nitrogen and oxygen are used as the sources for ozone profiles. Since the ratio of these two principal molecular constituents is constant to within 10 ppm in the lower atmosphere¹⁷, any variation in the vertical profile of a constant ratio can be associated with the integrated absorption due to ozone. The only

other species that has been found to be of concern at these wavelengths is SO_2 , and that we have observed in diesel exhaust plumes.¹⁶ Figure 2 shows the location of the Raman shifted wavelengths on the sloped side of the Hartley Band. Using the laboratory measured cross-sections in a DIAL lidar inversion analysis, the concentrations of ozone can be calculated.^{6,12} This technique eliminates the task of tuning and stabilizing the frequency and knowledge of the relative power of transmitted wavelengths as required for typical DIAL measurements. The fact that the nitrogen and oxygen molecules scatter a known fraction of the two Raman wavelengths in each volume element makes the technique a very robust measurement.

2.3. Optical Extinction Measurements

The extinction coefficient is made up of components due to absorption by chemical species and particles, and scattering by molecules and particles.¹⁸ The Raman scatter signals from the major molecular species provide direct measurements of the optical extinction. The direct backscatter signal at the transmitted wavelength exhibits a profile that combines the effects of molecular and particle scattering, and it is difficult to analyze and uniquely interpret for significant properties, except cloud height. However, analysis of the Raman profiles from molecular scattering signals provides unique vertical profiles of optical extinction. The LAPS instrument measures the optical extinction profiles from the gradients in each of the measured molecular profiles, at 607, 530 and 284 nm. The wavelength dependent optical extinction can be used to describe changes in the particle size distribution as a function of altitude for the important small particle sizes. These measurements can then be interpreted to determine the air mass parameter and atmospheric optical density. Measurements of optical extinction are based upon gradients in the molecular profiles, using the N_2 vibrational Raman scattering or a band of the rotational Raman lines. The calculation is easily applied to the rotational Raman signal at 530 nm because it is so close to the 532 nm transmitted wavelength that no wavelength dependence exists. By first calculating the extinction at 532 nm from the 530 nm path, it is possible to calculate the optical extinction at 607 nm without assuming a wavelength dependence for aerosol scattering.

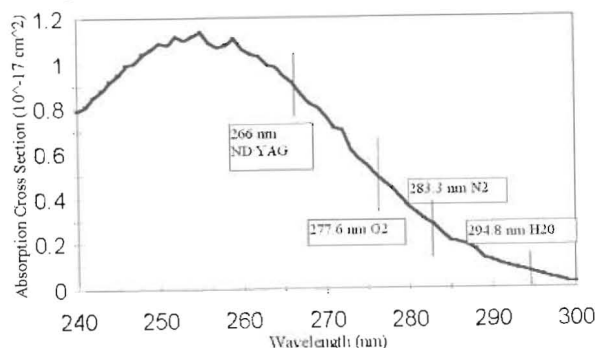


Figure 2. The absorption cross-section of the Hartley band of ozone is shown with the incident and scattered wavelengths indicated.¹⁹

3. LAPS INSTRUMENT

The LAPS lidar instrument has been developed from lessons learned during the development and use of five prior lidar instruments. The instrument was demonstrated as a first operational prototype lidar for the US Navy in 1996.^{16,20,22} The long term goal is to replace most of the current balloon sonde profiling and provide continuous routine measurements for future meteorological data. The shipboard testing of the Lidar Atmospheric Profile Sensor (LAPS) instrument demonstrated its ability to measure the principal atmospheric properties and capability for automated operation under a wide range of meteorological conditions. Raman lidar profiles are currently obtained at each minute, with a vertical resolution of 75 meters from the surface to 7 km. The LAPS instrument includes several sub-systems to automate the operation and provide the real-time results. Also, the instrument includes an X-band radar which detects aircraft as they approach the beam and automatically protects a 6 degree cone angle around the beam. Table 2 lists the primary characteristics of the LAPS lidar and Table 3 lists the measurements obtained and the typical altitude range and resolution of the data products expected.

Table 2. LAPS Lidar characteristics

Sub-System	Hardware	Properties
Transmitter	Continuum 9030 -- 30 Hz 5X Beam Expander	600 mj @ 532 nm 130 nj @ 266 nm
Receiver	61 cm Diameter Telescope	Fiber optic transfer
Detector	Seven PMT channels Photon Counting	528 and 530 nm -- Temperature 660 and 607 nm -- Water Vapor 294 and 285 nm -- Daytime Water Vapor 276 and 285 nm -- Raman/DIAL Ozone
Data System	DSP 100 MHZ	75 meter range bins
Safety Radar	Marine R-70 X-Band	protects 6° cone angle around beam

Table 3. Measurements made by the LAPS lidar instrument

Property	Measurement	Altitude	Time Resolution
Water Vapor	660/607 Raman 294/285 Raman	Surface to 5 km Surface to 3 km	Night - 1 min. Day & Night - 1 min.
Temperature	528/530 Rot. Raman	Surface to 5 km	Night (30 min.)
Ozone	276/285 Raman/DIAL	Surface to 2 - 3 km	Day and Night (30 min.)
Optical Extinction at 530 nm	530 nm Rot. Raman	Surface to 5 km	Night (10 to 30 min.)
Optical Extinction at 607 nm	607 N ₂ - I st Stokes	Surface to 5 km	Night (10 to 30 min.)
Optical Extinction at 285 nm	285 N ₂ - I st Stokes	Surface to 3 km	Day and Night (30 min.)

4. EXAMPLES OF RAMAN LIDAR RESULTS

The LAPS instrument uses Raman lidar techniques to simultaneously provide the profiles of water vapor, temperature, ozone and optical extinction. This paper introduces the measurements using examples from the recent applications of the Raman techniques for investigations of meteorological events and air quality episodes. The measurement campaigns which have been carried out to develop the present Raman lidar capability are listed in Table 4. The results presented here were obtained during the shipboard testing in 1996 on the USNS Sumner, during the Southern California Ozone Study SCOS97 and during a research program referred to as the North American Research Strategy for Tropospheric Ozone - Northeast - Oxidant and Particle Study (NARSTO-NE-OPS).²¹ The later program has been conducted by a consortium of universities and government laboratories and is focused on the air quality in the northeast urban corridor.

Table 4. Raman Lidar Measurement Campaigns

LADIMAS – RV Polarstern – Tromso, Norway to Antarctica – Oct 90-Jan 91
VOCAR – Pt Mugu CA – 1993, 1994
CASE – Wallops Island VA – Sept 1995
NARSTO-Northeast – Gettysburg PA – July 1996
USNS Sumner – Gulf of Mexico and Atlantic – Aug-Oct 1996
SCOS97 – Hesperia CA – Aug-Sept 1997
ARM and FIRE – Point Barrow AK – Feb-May 1998
NARSTO-NE-OPS – Philadelphia PA – August 1998
NARTSO-NE-OPS – Philadelphia PA – Jun-Aug 1999
NARSTO-NE-OPS – Philadelphia PA – Jun-Jul 2001

The primary measurement site for NE-OPS is located in Philadelphia, Pa and Figure 3 shows examples of profiles of water vapor and ozone. The water vapor profiles obtained with the LAPS instrument are shown together with measurements from a tethered sonde of Millersville University (Richard Clark) and aircraft measurements from the University of Maryland (Bruce Doddridge). These daytime water vapor measurements exhibit the variations typical of an active daytime convective boundary layer. The ozone profiles of the LAPS instrument and the University of Maryland aircraft are compared at night when the ozone profile is almost constant in the region of the residual boundary layer between 200 and 1700 meters. In the free troposphere, ozone patches can exist for relatively long periods of time and are frequently observed to drift in the background wind, and then be mixed down by convection to contribute to the next day surface layer concentrations. Within the thin nocturnal boundary layer, below 200-300 meters, the ozone is lost due to deposition and oxidation at the surface, together with some losses in surface layer chemical processes.

Figure 4 shows an example of the measurements obtained during the shipboard testing of the Raman lidar. Out over the Atlantic, the ozone was observed above the height of the marine boundary layer and was probably transported from production sources over the continent. The UV extinction is much larger than the visible component, as expected due to the larger cross-section for scattering from small particles. The optical extinction profiles are measured at both visible and ultraviolet wavelengths. It is interesting to note that the visible wavelength extinction exhibits a stronger correlation with water vapor content of the atmosphere, as would be expected for the hygroscopic sulfate and nitrate aerosols that are the dominant aerosol types in the eastern states. In Figure 4, the enhanced level of water vapor between 1 and 2.5 km correlates with a sub-visual cloud that was observed in both the visible and ultraviolet extinction profiles. Profiles presented as time sequences of the properties are much more useful for understanding the physical and chemical processes.

Several examples of lidar results have been selected from the Southern California Ozone Studies (SCOS97) which provide a range of interesting features. One feature observed several times was a plume of polluted air ejected from the Los Angeles basin, see Figures 5 and 6. The measuring site was located at Hesperia CA (at 1166 m elevation) in the high plateau at the east end of the Los Angeles basin. The results in Figures 5 and 6 show examples of a plume of polluted air being lofted up over our observation site. The plumes shown here, and in each of several other cases observed, demonstrate that high values of ozone, particulate matter and water vapor are strongly coupled. When a sea breeze, or a front, pushes the air at the coastal end of the basin, then polluted air that has accumulated at eastern end of the valley pushes up the mountain passes and spills out into the high plateau. Figure 6 shows a night and early morning period during relatively stable conditions. Under these stable conditions the ozone and water vapor concentrations are usually anti-correlated. However, the ejected plumes from the Los Angeles basin exhibit correlated increases in water vapor, ozone and optical extinction (ie. particulate matter), as would be expected for the stagnant polluted air mass in the Los Angeles area. The dynamical action that results in launching the plumes observed in these data sets appears to be effective in transporting the primary pollutant materials into the region. One point worth noting is that the ozone concentrations aloft and those at the surface are rarely directly coupled, and therefore use of surface measurements, the constructed models of air quality variations may not be too realistic. The nighttime residual layer is observed to frequently contain significant quantities of ozone, at altitudes above the nocturnal boundary layer, and this region can act as a storage reservoir for transport of additional ozone to the surface on the next day.

Figure 7 shows an interesting time sequence of the specific humidity profiles on 18 September 1997 when aircraft and radiosonde profiles are available for comparisons with the Raman lidar profiles. The aircraft data were obtained by Prof. John Carroll of the University of California at Davis as he made a spiral around the vertically pointed lidar beam. The aircraft measurements were taken as the plane climbed or descended on the legs of a 2 km square box that was centered on the vertically pointed lidar beam. The several comparisons between the aircraft and lidar data showed good agreement. This figure shows two of the time periods when direct comparison between the lidar and aircraft was made. The last panel on the right-hand side of Figure 7 shows how the profiles measured by a radiosonde balloon can be misleading. The balloon flight is represented by a line on the graph that shows the approximate altitude versus time profile. A rather striking feature is observed at 1.5 km where the flight of the balloon takes it through a narrow region which was depleted in water vapor. The time resolved lidar profiles provide a very clear reason for the profile feature, and demonstrates the importance of continuous profiles. Also, the gradient of the water vapor in the 2.5 to 3 km range agrees well with the water vapor measured by the lidar at the time when the balloon passed through that region. These results graphically demonstrate that a single balloon profile can mislead the observer concerning the actual conditions present in the atmosphere.

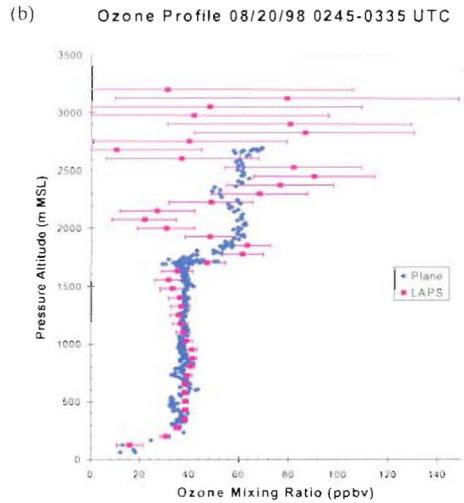
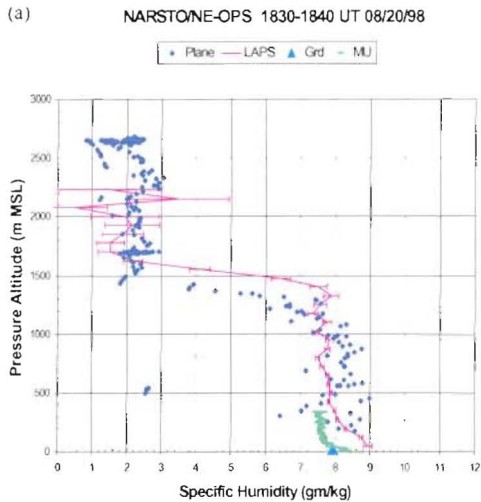


Figure 3. Examples of three sets of profiles measured by the LAPS lidar as part of the NARSTO-NE-OPS program in Philadelphia during August 1998. (a) The water vapor measurements from LAPS lidar, the Millersville University tether sonde (R. Clark), and University of Maryland aircraft (B. Doddridge) are compared. (b) An ozone profile of the LAPS lidar is compared with the University of Maryland aircraft.

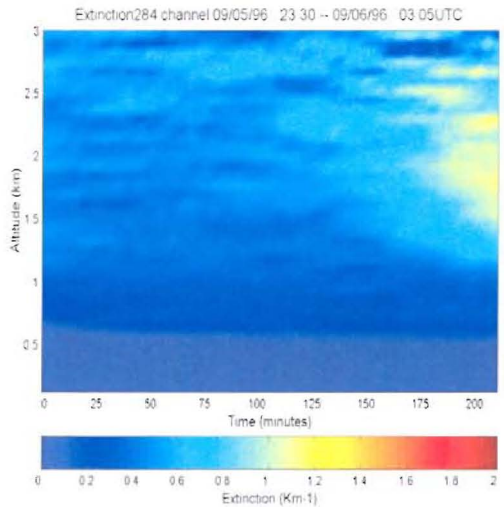
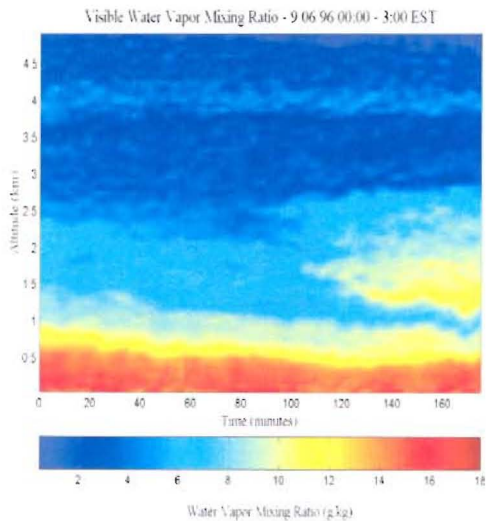


Figure 4. An example of water vapor and optical extinction measurements from tests on the USNS Sumner during the development of a sub-visual cloud between 1 and 2.5 km on 6 September 1996.

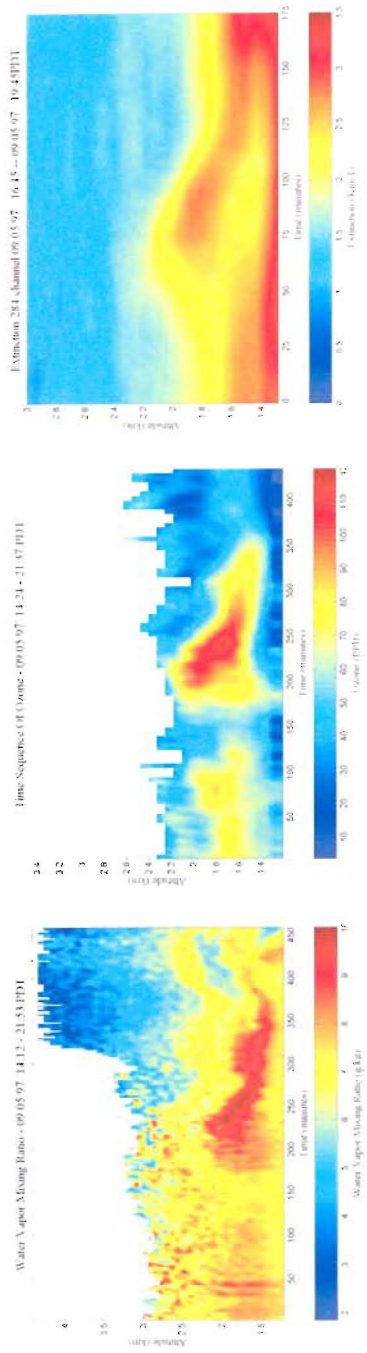


Figure 5. The water vapor, ozone and optical extinction time sequence profiles are shown during the period when a plume of polluted air from the Los Angeles basin drifts over the SCOS site at Hesperia, CA on 5 Sept 1997. The water vapor plots are shown for one minute time steps with 5 minute filter width and the ozone and extinction are shown with 10 minute time steps and 30 minute filter.

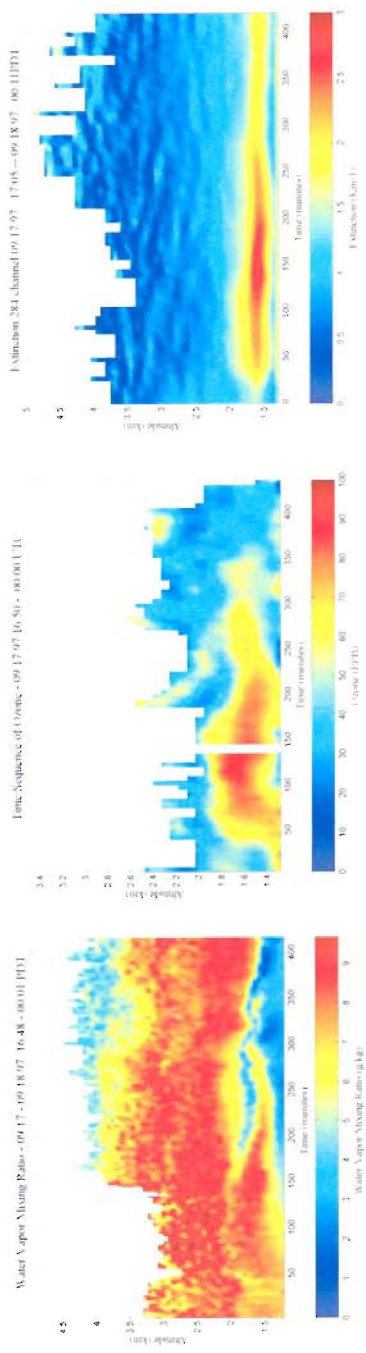


Figure 6. The water vapor, ozone and optical extinction time sequence profiles show a plume of air pollution lofted from Los Angeles into the atmosphere above the high plateau at the east end of the L.A basin on 17 September 1997.

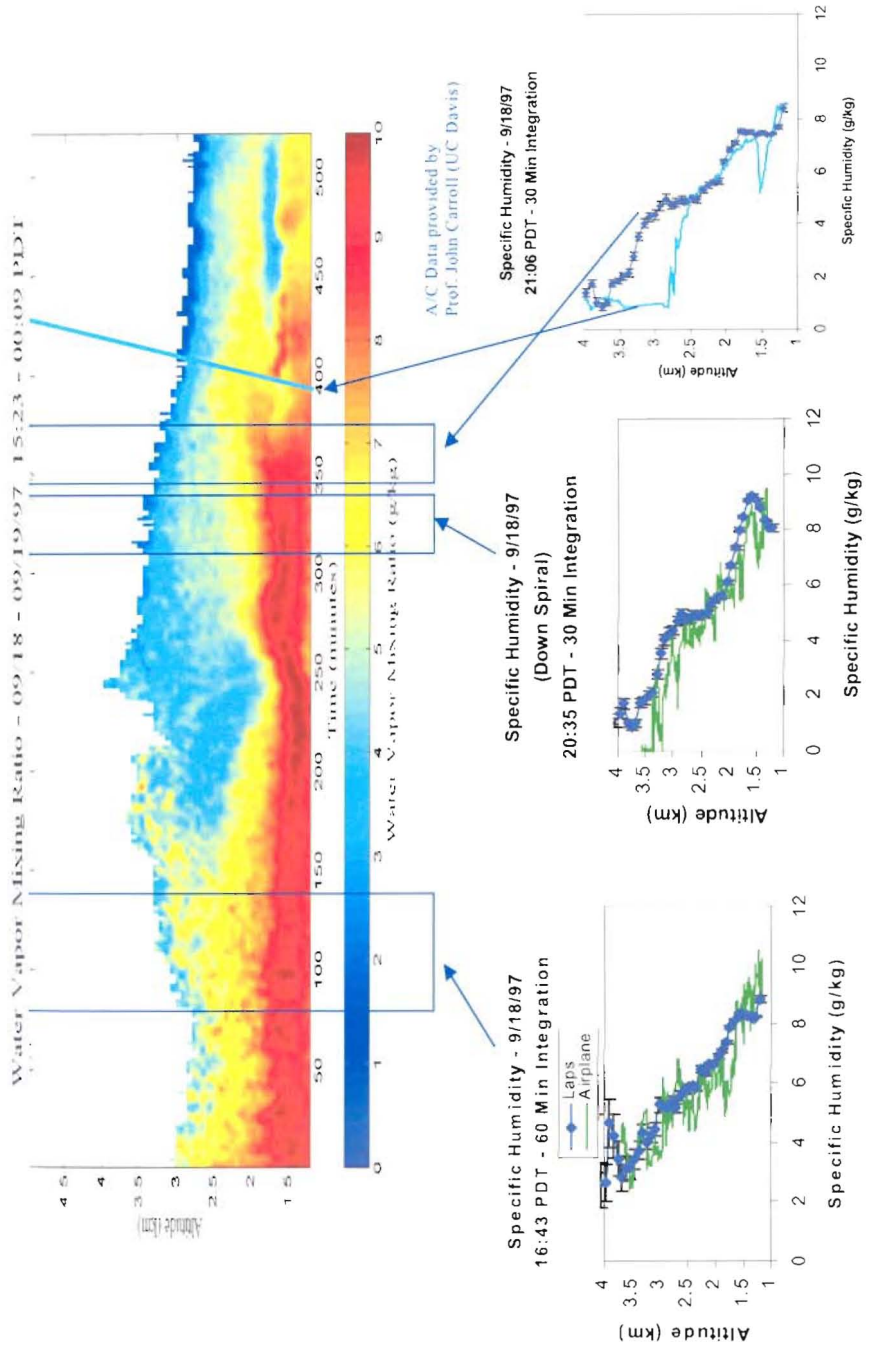


Figure 7. The time sequence of the Raman lidar profiles of water vapor are shown together with aircraft sensor measurements and a radiosonde profile for comparison. The aircraft profiles (J. Carroll, UC Davis) and lidar show good agreement and any differences can be correlated with features observed in the profile time sequences. The radiosonde profile demonstrates the limitations of a single balloon profile compared with the complete picture provided by the lidar

5. CONCLUSIONS

Raman lidar measurements provide the key results for understanding the physical/chemical processes associated with meteorological processes and air pollution episodes. The primary goals of the research undertaken in the environmental programs are to investigate, understand and model the physical and chemical processes important in evolution of air pollution events. By measuring the details of the species concentrations and the meteorological factors controlling transport, it is possible to identify the local and distant sources that contribute to increased concentrations of ozone and PM_{2.5}. Additional health physics studies attempt to connect the sources of air pollution with population exposure and health effects. Finally, these results are used to test and develop models which will be used in the future for meteorological and air quality forecasting. The goal of the air quality community is to fully predict the distribution of air pollutants provide a capability to test regulatory measures. These measurement programs also provide an opportunity to improve and validate new measuring techniques needed for process monitoring.

Measurements of the variations in the profiles of optical extinction, water vapor, and ozone provide valuable insight into the evolution of pollution events. Raman lidar measurements show the effects of dynamical processes occurring in the lower atmosphere and demonstrate the importance of using higher resolution measurements to examine vertical mixing, horizontal transport, and distribution of water vapor, chemical species and particulate materials in an elevated layer. The details revealed in the time sequences of the lidar data add a new dimension to understanding meteorological processes and the evolution of air pollution episodes. The vertical profile information and temporal variations are expected to provide the critical tests for the models under development. The continuous vertical profiles that can be obtained using lidar provide an important dimension for investigating the physical and chemical process of the atmosphere. Combining the Raman lidar with other measurements, such as Doppler radar, provides the complete set of parameters needed for testing model predictions, evaluating dynamical processes (vertical and horizontal), investigating turbidity, obtaining optical extinction profiles. Raman lidar appears to provide the best solution for upgrading the capability of the primary data to describe the meteorology of the lower atmosphere with improved temporal and spatial resolution. The measurement capabilities have been demonstrated and the Raman lidar approach has been found to be attractive both technically and economically.

6. ACKNOWLEDGMENTS

This work is supported by the US EPA grant titled 'Investigations of Factors Determining the Occurrence of Ozone and Fine Particles in Northeastern USA,' grant number R826373. The PSU lidar development, shipboard testing, and evaluation at several field sites have been supported by the US Navy through SPAWAR Systems Division - San Diego, PMW-185, NAVOCEANO, NAWC Point Mugu, ONR, DOE, EPA, CARB, NASA and NSF. The efforts of George Allen of Harvard School of Public Health, Richard Clark of Millersville University, Russell Dickerson and Bruce Doddridge of University of Maryland, S.T. Rao of NY State Dept. of Environmental Conservation, Ted Erdman of EPA Region 3, Bill McClenny, Ken Schere and Robin Dennis of USEPA, Susan Weirman of MARAMA, Jerry Lentz of Marina Photonics, Bart Croes and Leon Dolislager of CARB, and at Penn State University, William Ryan, Dan Lysak, Tom Petach, Ed Novitsky, Guangkun Li, Alexander Achey, Gregg O'Marr, Karoline Mulik, Steven Esposito, Alex Achey, Corey Slick, and Sriram Kizhakkemadam have contributed much to the success of this project.

7. REFERENCES

1. Magari, S.R., R. Hauser, J. Schwartz, P.L. Williams, T.J. Smith, D.C. Christiani, "Association of Heart Rate Variability with Occupational and Environmental Exposure to Particulate Air Pollution," *Circulation* **104**, 986-991, 2001.
2. Peters, A., D.W. Dockery, J.E. Muller and M.A. Mittleman, "Increased Particulate Air Pollution and the Triggering of Myocardial Infarction," *Circulation* **103**, 2810-2815, 2001.
3. Mauderly, Joe, Lucas Neas, and Richard Schlesinger, "PM Monitoring Needs Related to Health Effects", *Proceedings of the PM Measurements Workshop*, EPA Report No. 2, Chapel Hill, North Carolina, pp 9-14, July 1998.
4. Albritton, Daniel L., and Daniel S. Greenbaum, "Atmospheric Observations: Helping Build the Scientific Basis for Decisions Related to Airborne Particle Matter", *Proceedings of the PM Measurements Research Workshop*, EPA Report No. 1, Chapel Hill, North Carolina, pp. 1-8, July 22-23, 1998.
5. Hidy, G. M., P. M. Roth, J. M. Hales and R. Scheffe, "Oxidant Pollution And Fine Particles: Issues And Needs," NARSTO Critical Review Series, 1998, <http://odyssey.owt.com/Narsto/>
6. Philbrick, C.R., "Raman Lidar Measurements of Atmospheric Properties", *Atmospheric Propagation and Remote Sensing III*, SPIE Vol. 2222, 922-931, 1994.
7. Balsiger, F., and C. R. Philbrick, "Comparison of Lidar Water Vapor Measurements Using Raman Scatter at 266nm and 532 nm," in *Applications of Lidar to Current Atmos. Topics*, SPIE Proc. Vol. 2833, 231-240 1996.
8. Balsiger, F., P. A. T. Haris and C. R. Philbrick, "Lower-tropospheric Temperature Measurements Using a Rotational Raman Lidar," in *Optical Instruments for Weather Forecasting*, SPIE Proc. Vol. 2832, 53-60, 1996.
9. Haris, P.A.T., "Pure Rotational Raman Lidar for Temperature Measurements in the Lower Troposphere," PhD Thesis for Penn State University, Department of Electrical Engineering, August 1995.
10. Esposito, S.T., and C.R. Philbrick, "Raman/DIAL Technique for Ozone Measurements," *Proceeding of Nineteenth International Laser Radar Conference*, NASA/CP-1998-207671/PT1, pp 407-410, 1998.
11. Philbrick, C.R., "Raman Lidar Capability to Measure Tropospheric Properties," *Proceeding of Nineteenth International Laser Radar Conference*, NASA/CP-1998-207671/PT1, pp 289-292, 1998.
12. O'Brien, M.D., T. D. Stevens and C. R. Philbrick, "Optical Extinction from Raman Lidar Measurements," in *Optical Instruments for Weather Forecasting*, SPIE Proceedings Vol. 2832, 45-52, 1996.
13. Philbrick, C.R., M. D. O'Brien, D. B. Lysak, T. D. Stevens and F. Balsiger, "Remote Sensing by Active and Passive Optical Techniques," *NATO/AGARD Proceedings on Remote Sensing*, AGARD-CP-582, 8.1-8.9, 1996.
14. Philbrick, C.R., D.B. Lysak, Jr., M. O'Brien and D.E. Harrison, "Lidar Measurements of Atmospheric Properties," in *Proceedings of the Electromagnetic/Electro-Optics Performance Prediction and Products Symposium*, Naval Post Graduate School, Monterey CA, 385-400, June 1997.
15. Philbrick, C.R., and D.B. Lysak, Jr., "Atmospheric Optical Extinction Measured by Lidar," *Proceedings of the NATO-SET Panel Meeting on E-O Propagation*, NATO RTO-MP-1, pp.40-1 to 40-7, 1998.
16. Philbrick, C.R., and D. B. Lysak, Jr., "Optical Remote Sensing of Atmospheric Properties," *Proceedings of the Battlespace Atmospheric and Cloud Impacts on Military Operations (BACIMO)*, Air Force Research Laboratory, AFRL-VS-HA-TR-98-0103, pg 460-468, 1999.
17. Sedlacek, III, A.J., M.D. Ray and M. Wu, "Augmenting Classical DIAL with Raman-DIAL (RaDIAL)," in *Application of Lidar to Current Atmospheric Topics III*, SPIE Proc. Vol.3757, 126-139, 1999.
18. Measures, Raymond M., *Laser Remote Sensing*, Wiley-Interscience, New York: 1984.
19. Inn, E.C., and Y. Tanaka, "Absorption Coefficient of Ozone in the Ultraviolet and Visible Regions," *J. Optical Society*, **43**, 870-873, 1953.
20. Philbrick, C.R., and D. B. Lysak, Jr., "Lidar Measurements of Meteorological Properties and Profiles of RF Refractivity," *Proceedings of the 1996 Battlespace Atmospherics Conference*, Technical Document 2938 NCCOSC RDT&E, pg 595-609, 1996.
21. Philbrick, C.R., "Investigations of Factors Determining the Occurrence of Ozone and Fine Particles in Northeastern USA," *Proceedings of Symposium on Measurement of Toxic and Related Air Pollutants*, Air & Waste Management Association, pp 248-260, 1998.
22. Philbrick, C.R. and K Mulik, "Application of Raman Lidar to Air Quality Measurements," *Proceedings of the SPIE Conference on Laser Radar Technology and Applications V*, pp 22-33, 2000.